

## Structural and Electronic Behavior of Unprecedented Five-Coordinate Iron(III) and Gallium(III) Complexes with a New Phenol-Rich Electroactive Ligand

Mauricio Lanznaster,<sup>†,‡</sup> Hrant P. Hrachian,<sup>†,§</sup> Mary Jane Heeg,<sup>†</sup> Lew M. Hryhorczuk,<sup>†</sup> Bruce R. McGarvey,<sup>||</sup> H. Bernhard Schlegel,<sup>†</sup> and Claudio N. Verani<sup>\*,†</sup>

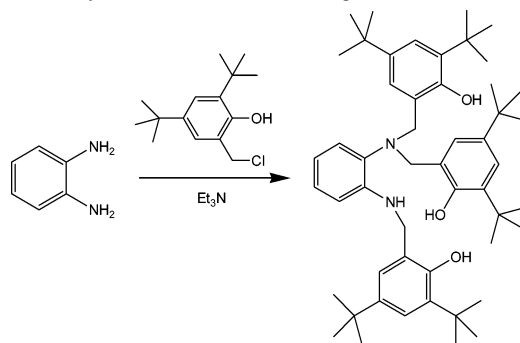
Department of Chemistry, Wayne State University, Detroit, Michigan 48202, and Department of Chemistry, University of Windsor, Windsor, Ontario N9B 1P4, Canada

Received May 19, 2005

A new asymmetric pentadentate ligand was designed to impose low symmetry to trivalent ions. Five-coordinate  $\text{Fe}^{3+}$  and  $\text{Ga}^{3+}$  complexes were investigated by crystallographic, electrochemical, and electron paramagnetic resonance methods showing enhanced redox reversibility. Calculations were performed to account for the observed trends.

Several current advances in nanoscience depend on the development of molecular materials with customized and controlled properties. Synthetic chemistry plays a unique role in delivering such materials and molecules that can act as switches are expected to have significant potential for information technology.<sup>1</sup> Therefore, molecular magnetic materials are receiving increasing attention,<sup>2</sup> when the requirements of response to an external stimulus and bistability are fulfilled.<sup>3</sup> Transition-metal complexes with electroactive ligands able to support the generation and stabilization of organic radicals are of special interest.<sup>4</sup> Among the well-characterized redox-active systems, phenoxyl radi-

**Scheme 1.** Synthesis of the New  $\text{N}_2\text{O}_3$  Ligand **H<sub>3</sub>L**



cals resulting from phenolate oxidation can be generated in pseudo-octahedral complexes,<sup>5</sup> but the remarkable redox reversibility seen in biological systems cannot be matched. In nature the phenolate/phenoxyl couple is bound to five-coordinate ions, and this environment might be responsible for the observed redox versatility. Thus, ligand design can be used to foster unusual geometries in trivalent metal centers and may enhance stable switching mechanisms. In this account, we report the design and structural data on five-coordinate complexes  $[\text{M}^{\text{III}}\text{L}]$  containing trivalent iron and gallium ions surrounded by an  $\text{N}_2\text{O}_3$  coordination sphere in which phenolate groups are capable of supporting the formation of up to three phenoxyl radicals. Electrochemical data support an improved reversibility of the ligand-centered redox processes and suggest that unusual magnetic interactions between metal and radicals may take place.

The new ligand **H<sub>3</sub>L** was synthesized according to Scheme 1 and treated with  $\text{FeCl}_3$  and  $\text{GaCl}_3$ , yielding  $[\text{Fe}^{\text{III}}\text{L}]$  (**1**) and  $[\text{Ga}^{\text{III}}\text{L}]$  (**2**), respectively. The five-coordination mode has been observed by electrospray ionization (ESI) spectrometry in methanol by both peak position and isotopic distribution, as well as via elemental analysis in the solid

\* To whom correspondence should be addressed. E-mail: cverani@chem.wayne.edu.

<sup>†</sup> Wayne State University.

<sup>‡</sup> Present address: Institute of Chemistry, Universidade Federal Fluminense, Niterói, RJ 24020, Brazil.

<sup>§</sup> Present address: Department of Chemistry, Indiana University, Bloomington, IN 47405.

<sup>||</sup> University of Windsor.

- (1) (a) Dei, A.; Gatteschi, D.; Sangregorio, C.; Sorace, L. *Acc. Chem. Res.* **2004**, *37*, 827. (b) Kahn, O.; Martinez, C. J. *Science* **1998**, *279*, 44. (c) Verdager, M. *Science* **1996**, *272*, 698.
- (2) (a) Holten, D.; Bocian, D. F.; Lindsey, J. S. *Acc. Chem. Res.* **2002**, *35*, 57. (b) Wolf, S. A.; Awshalom, D. D.; Buhman, R. A.; Daughton, J. M.; Molnar, S.; Roukes, M. L.; Chitchekanova, A. Y.; Treger, D. M. *Science* **2001**, *294*, 1488.
- (3) (a) Marchivie, M.; Guionneau, P.; Howard, J.; Chastanet, G.; Letard, J.-F.; Goeta, A.; Chasseau, D. *J. Am. Chem. Soc.* **2002**, *124*, 194. (b) Pease, A. R.; Jeppesen, J. O.; Stoddart, J. F.; Luo, Y.; Collier, C. P.; Heath, J. R. *Acc. Chem. Res.* **2001**, *34*, 433. (c) Fabbrizzi, L.; Licchelli, M.; Pallavicini, P. *Acc. Chem. Res.* **1999**, *32*, 846.
- (4) (a) Hicks, R. G.; Lemaire, M. T.; Thompson, L. K.; Barclay, T. M. *J. Am. Chem. Soc.* **2000**, *122*, 8077. (b) Kahn, O. *Acc. Chem. Res.* **2000**, *33*, 647. (c) Miller, J. S. *Inorg. Chem.* **2000**, *39*, 4392. (d) Aukauloo, A.; Ottenwaelder, X.; Ruiz, R.; Poussereau, S.; Pei, Y.; Journaux, Y.; Fleurat, P.; Volatron, F.; Cervera, B.; Muñoz, M. C. *Eur. J. Inorg. Chem.* **1999**, *7*, 106.

- (5) (a) Pratt, R. C.; Mirica, L. M.; Stack, T. D. P. *Inorg. Chem.* **2004**, *43*, 8030 and references cited therein. (b) Chaudhuri, P.; Wieghardt, K. *Prog. Inorg. Chem.* **2001**, *50*, 151. (c) Jadzewski, B. A.; Tolman, W. B. *Coord. Chem. Rev.* **2000**, *200–202*, 633.

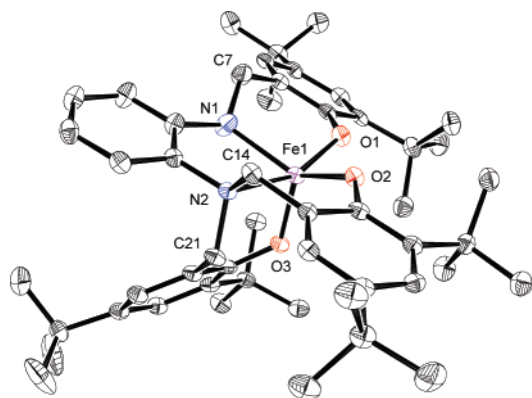


**Figure 1.** ORTEP view of **1**. Selected bond distances (Å) and angles (deg): Fe1–O1 = 1.887(1), Fe1–O2 = 1.868(1), Fe1–O3 = 1.871(1), Fe1–N1 = 2.148(2), Fe1–N2 = 2.233(2), C7–N1 = 1.414(3), O1–Fe1–N2 = 158.67(6), O2–Fe1–O3 = 115.98(6), O2–Fe1–N1 = 140.92(7), O3–Fe1–N1 = 101.09(7), N1–Fe1–N2 = 77.40(6), O2–Fe1–N2 = 88.75(6), O3–Fe1–N2 = 92.20(6), N1–Fe1–O1 = 87.96(6), O2–Fe1–O1 = 93.15(6), O3–Fe1–O1 = 105.93(6).

state, and has been confirmed by electron paramagnetic resonance (EPR) and single-crystal X-ray diffraction.

X-ray data reveal two independent molecules in the unit cell of **1**<sup>6</sup> differing slightly in their parameters. The ORTEP view and selected bond lengths and angles of **1** are shown in Figure 1.

The Fe<sup>3+</sup> ion is surrounded by three phenolate oxygen atoms and two amine nitrogen atoms of L<sup>3-</sup>. The oxygen O2 and O3 and the nitrogen N1 atoms form a trigonal plane around the metal center, whereas the remaining oxygen O1 and nitrogen N2 atoms lie at the apical positions of the distorted trigonal bipyramid. Although a trigonal-bipyramidal geometry was defined, a square pyramid could also be used to describe the geometry of L<sup>3-</sup> around the Fe<sup>3+</sup> center considering the calculated values for the degree of trigonality<sup>7</sup>  $\tau = 0.29$  and  $0.53$  for the two molecules in **1**. In general, the Fe–N and Fe–O bond distances are in the range of those reported for other Fe<sup>3+</sup> complexes containing related ligands.<sup>8</sup> The molecular structure of **2** was also determined<sup>9</sup> and shows a five-coordinate arrangement of L<sup>3-</sup> around the gallium ion

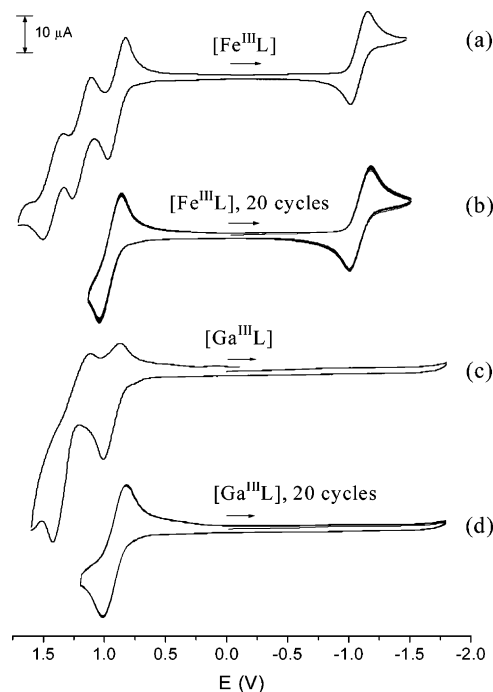


**Figure 2.** CVs of [Fe<sup>III</sup>L] and [Ga<sup>III</sup>L] at  $2.0 \times 10^{-3}$  mol L<sup>-1</sup> in CH<sub>2</sub>Cl<sub>2</sub> with 0.1 mol L<sup>-1</sup> TBAPF<sub>6</sub>, at 0.1 V s<sup>-1</sup> at room temperature using a three-electrode system (W = carbon, Ref. = Ag/AgCl, Aux. = Pt wire). Ferrocene was used as an internal standard ( $E_{1/2} = 0.46$  V).

( $\tau = 0.57$ ) similar to that observed for **1**. The average Ga–O and Ga–N bond lengths are respectively 0.026 and 0.066 Å smaller than the corresponding distances for the iron complex (Figure S1 in the Supporting Information).

The cyclic voltammogram (CV) of **1** (Figure 2) exhibits a one-electron process at  $E_{1/2} = -1.44$  V vs Fc<sup>+/0</sup>, which is assigned to the Fe<sup>III</sup>/Fe<sup>II</sup> couple. This value is on average 0.4 V less negative when compared with the metal-centered process seen for N<sub>3</sub>O<sub>3</sub>–Fe<sup>III</sup> complexes containing three phenolate groups.<sup>10</sup> As expected, no cathodic peak was found associated with the gallium(III) ion. Nonetheless, two anodic waves are observed at 0.47 and 0.81 V vs Fc<sup>+/0</sup> for **2**, and three waves at 0.51, 0.77, and 0.99 V vs Fc<sup>+/0</sup> are observed for **1** (Figure 2). These processes are attributed to the oxidation of the phenolate groups in L<sup>3-</sup>, thus generating phenoxy radical species.<sup>11</sup> The potentials agree with the observed ligand-centered waves at 0.38, 0.65 and 0.96 (irr) V vs Fc<sup>+/0</sup> in a six-coordinate iron complex with the tris-(di-*tert*-butylphenol)triazacyclononane ligand.<sup>10b</sup> It is suggested that the more positive wave at 0.78 V for **2** (Figure

(6) Crystal data for [Fe<sup>III</sup>L]: C<sub>51</sub>H<sub>71</sub>FeN<sub>2</sub>O<sub>3</sub>, 815.95; triclinic,  $P\bar{1}$ ;  $a = 15.1273(3)$  Å,  $b = 15.7187(3)$  Å,  $c = 21.6951(4)$  Å;  $\alpha = 73.9620(10)^\circ$ ,  $\beta = 83.6280(10)^\circ$ ,  $\gamma = 75.3460(10)^\circ$ ;  $V = 4791.95(16)$  Å<sup>3</sup>;  $Z = 4$ ;  $T = 100(2)$  K;  $\lambda = 0.71073$  Å;  $D_{\text{calcd}} = 1.131$  mg/m<sup>3</sup>,  $\mu = 0.355$  mm<sup>-1</sup>;  $R(F) = 3.63\%$ ,  $wR(F) = 7.89\%$ .

(7)  $\tau = (\beta - \alpha)/60$ , where  $\beta$  is the largest angle and  $\alpha$  is the second-largest angle in the coordination sphere. See: Addison, A. W.; Rao, T. N. *J. Chem. Soc., Dalton Trans.* **1984**, 1349.

(8) (a) Imbert, C.; Hratchian, H. P.; Lanznaster, M.; Heeg, M. J.; Hryhorczuk, L. M.; McGarvey, B. R.; Schlegel, H. B.; Verani, C. N. *Inorg. Chem.* **2005**, *44*, 7414. (b) Fujii, H.; Funahashi, Y. *Angew. Chem., Int. Ed.* **2002**, *41*, 3638. (c) Lanznaster, M.; Neves, A.; Bortoluzzi, A. J.; Szpoganicz, B.; Schwingel, E. *Inorg. Chem.* **2002**, *41*, 5641. (d) Verani, C. N.; Bothe, E.; Burdinski, D.; Weyhermuller, T.; Florke, U.; Chaudhuri, P. *Eur. J. Inorg. Chem.* **2001**, *8*, 2161. (e) Setyawati, I. A.; Rettig, S. J.; Orvig, C. *Can. J. Chem.* **1999**, *77*, 2033. (f) Hwang, J.; Govindaswamy, K.; Koch, S. A. *Chem. Commun.* **1998**, 1667.

(9) Crystal data for [Ga<sup>III</sup>L]: C<sub>53</sub>H<sub>73</sub>Cl<sub>6</sub>N<sub>2</sub>O<sub>3</sub>Ga<sub>1</sub>, 1068.55; monoclinic,  $P2_1/c$ ;  $a = 16.2891(8)$  Å,  $b = 18.0037(9)$  Å,  $c = 20.2754(10)$  Å;  $\beta = 112.814(2)^\circ$ ;  $V = 5480.9(5)$  Å<sup>3</sup>;  $Z = 4$ ;  $T = 100(2)$  K;  $\lambda = 0.71073$  Å;  $D_{\text{calcd}} = 1.295$  mg m<sup>-3</sup>,  $\mu = 0.836$  mm<sup>-1</sup>;  $R(F) = 6.84\%$ ,  $wR(F) = 17.20\%$ . Selected bond lengths (Å) and angles (deg): Ga–O1 = 1.867(3), Ga–O2 = 1.833(3), Ga–O3 = 1.839(3), Ga–N1 = 2.092(4), Ga–N2 = 2.172(3), O1–Ga–N2 = 165.78(13), O2–Ga–

O3 = 112.98(12), O2–Ga–N1 = 131.81(13), O3–Ga–N1 = 114.84(14), N1–Ga–N2 = 80.42(13), O2–Ga–N2 = 91.39(12), O3–Ga–N2 = 93.32(12), N1–Ga–O1 = 87.68(13), O2–Ga–O1 = 90.78(12), O3–Ga–O1 = 98.76(13).

(10) (a) Nairn, A. K.; Bhalla, R.; Foxon, S. P.; Liu, X.; Yellowlees, L. J.; Gilbert, B. C.; Walton, P. H. *J. Chem. Soc., Dalton Trans.* **2002**, 1253. (b) Adam, B.; Bill, E.; Bothe, E.; Goerd, B.; Haselhorst, G.; Hildenbrand, K.; Sokolowski, A.; Steenken, S.; Weyhermuller, T.; Wieghardt, K. *Chem.–Eur. J.* **1997**, *3*, 308.

(11) (a) Benisvy, L.; Blake, A. J.; Collison, D.; Davies, E. S.; Garner, C. D.; McInnes, E. J. L.; McMaster, J.; Whittaker, G.; Wilson, C. *J. Chem. Soc., Dalton Trans.* **2003**, 1975. (b) Maki, T.; Araki, Y.; Ishida, Y.; Onomura, O.; Matsumura, Y. *J. Am. Chem. Soc.* **2001**, *123*, 3371. (c) Hammerich, O.; Svensmark, B. In *Organic Electrochemistry*; Henning, L., Baizer, M. M., Eds.; Marcel Dekker: New York, 1991; pp 615–657.

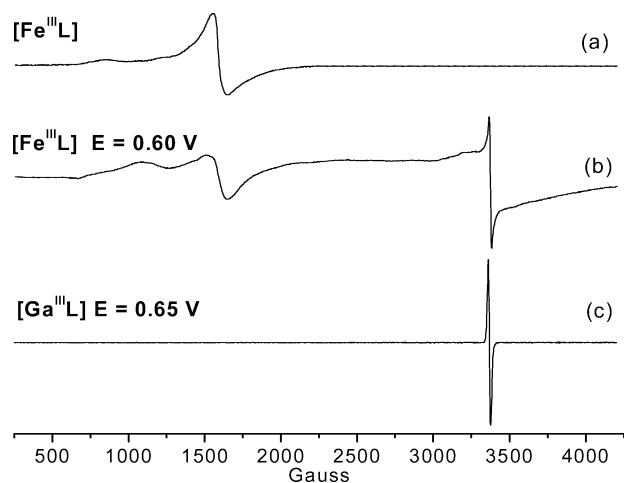


**Figure 3.** X-band EPR at 120 K from  $1 \times 10^{-3}$  mol L $^{-1}$  frozen solutions of **1** before (a) and after (b) electrolysis at 0.60 V vs Fc $^{+}$ /Fc and **2** after electrolysis at 0.65 V vs Fc $^{+}$ /Fc (c), in dichloromethane/TBAPF $_6$  (0.1 mol L $^{-1}$ ).

2c) is an overlap of two redox processes. At  $-30$  °C in MeCN (Figure S2 in the Supporting Information), this assignment unfolds in three cathodic waves at 0.52, 0.67, and 0.89 V vs Fc $^{+}$ /Fc. An attempt to evaluate the reversibility of the phenolate/phenoxyl couples in **1** and **2** was performed by cycling 20 times through the wave associated with the first ligand-centered process. This cycling simulates a switching mechanism (Figure 2b,d). No current decay was detected, thus indicating that decomposition of the generated species in the time scale of the voltammetry did not take place. It suggests that the phenoxyl species are stable when under a five-coordinate geometry in noncoordinating solvents. Only minor current changes were observed when full-range CVs including all of the anodic processes were scanned.

The EPR spectrum of **1** shows a large signal at  $g = 4.26$  expected for a high-spin Fe $^{3+}$ -containing species and a small peak at  $g = 8.3$  (Figure 3a). The zero-field parameters  $D$  and  $E$  are used to assess the electrical symmetry around the iron center, with the magnitude of  $E$  being found within 0 and  $|D/3|$ . A maximum deviation from axial symmetry is obtained when  $E = D/3$ . Examination of a series of simulated spectra with varying  $D$  and  $E$  (Figure S3 in the Supporting Information) suggests that a single peak at  $g = 4.26$  requires  $D \geq 3000$  G and  $E$  near  $D/3$ . The turning point seen at about 800 G becomes more prominent when  $E$  is slightly less than  $D/3$ . This spectrum supports a highly distorted nature of the compound in solution, thus in good agreement with its solid X-ray crystal structure.

The product of the first oxidation of **1** shows a signal at  $g = 2.00$  attributed to phenoxyl radical species along with substantial changes in the shape of the iron-related signal. A new turning point around 1100–1200 G indicates the presence of a different Fe $^{3+}$  site with a lower  $E$  value relative to  $D$ , suggesting increased symmetry, possibly related to six-coordination. Despite the relative reversibility of post-electrolysis CVs, the ESI spectrum of the electrolyzed solution is complex, with new peaks being present along with **1**. Although the differences in the intensity and shape of the

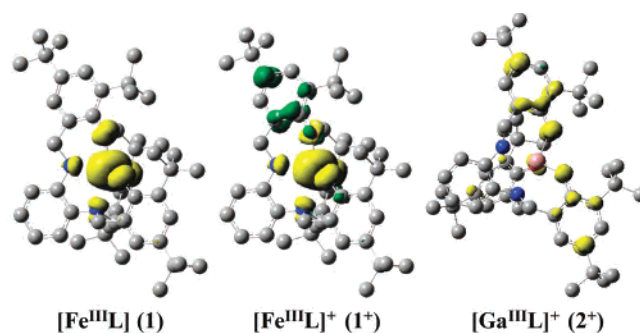


**Figure 4.** Spin-density plot for **1** (left), **1** $^{+}$  (center), and **2** $^{+}$  (right). The yellow color indicates excess  $\alpha$  electron density, whereas the green color indicates excess  $\beta$  electron density. Hydrogen atoms were omitted for clarity.

Fe $^{3+}$  signal may imply unusual metal/radical couplings, we refrain from discussing these interactions at this time. A signal at  $g = 2.00$  (Figure 3c) has been observed for the product of the first oxidation of **2** and is attributed to the formation of a phenoxyl radical.

Density functional theory calculations have been carried out on **1** and **2** to study the electronic structure of these compounds and their mono-, bi-, and trivalent cations, generated upon radical formation. Spin-density plots for **1**, **1** $^{+}$ , and **2** $^{+}$  are shown in Figure 4. An antiferromagnetic coupling is predicted to be the more stable configuration for **1** $^{+}$ . Consistent with the high-spin 3d $^5$  configuration of the iron(III) center, excess  $\alpha$  spin density is centered on the metal atom for **1**. The plots for **1** $^{+}$  and **2** $^{+}$  indicates that oxidation results in radical formation on the phenolate rings.

A slow conversion of the secondary amine group to the corresponding imine was observed via ESI spectrometry for both **1** and **2**, as seen recently for similar systems.<sup>12</sup> The characterization of these species and a detailed study on the EPR properties of these systems will be the subject of a future paper.

In summary, we have developed a new pentadentate electroactive ligand capable of stabilizing five-coordinate iron(III) and gallium(III) complexes. Phenoxyl radicals can be generated for both compounds, and the first ligand-centered oxidative process can be reversibly cycled without apparent structural changes. This result points out the potential relevance of these compounds as ground-state switches.

**Acknowledgment.** C.N.V. thanks the Wayne State University, the donors of the American Chemical Society Petroleum Research Fund (Grant 42575-G3), and the Nano@Wayne initiative (Grant 11E420) for financial support. H.B.S. thanks the National Science Foundation (Grant CHE 0131157), and H.P.H. thanks the WSU-Institute for Scientific Computing for an NSF-IGERT fellowship.

**Supporting Information Available:** Experimental details, calculations, and X-ray crystallographic data (CIF). This material is available free of charge via the Internet at <http://pubs.acs.org>. IC050809I

(12) Machkour, A.; Mandon, D.; Lachkar, M.; Welter, R. *Eur. J. Inorg. Chem.* **2005**, *1*, 158.